Verification of Single Beam Treatment Planning Using a Ferrous Dosimeter Gel and MRI (FeMRI)

Sven Å.J. Bäck, Peter Magnusson, Lars E. Olsson, Anders Montelius, Annette Fransson and Sören Mattsson

From the Department of Radiation Physics, Malmö, Lund University, Malmö University Hospital, Sweden (S.Å.J. Bäck, P. Magnusson, L.E. Olsson, S. Mattsson), Department of Hospital Physics, University Hospital, Uppsala, Sweden (A. Montelius, A. Fransson) and Department of Biomedical Engineering and Physics, University of Vienna, Austria (A. Fransson)

Correspondence to: Sven Å.J. Bäck, Department of Radiation Physics, Lund University, Malmö University Hospital, SE-205 02 Malmö, Sweden. Tel: +46 40 33 25 01. Fax: +46 40 96 31 85. E-mail: sven.back@rfa.mas.lu.se

Acta Oncologica Vol. 37, No. 6, pp. 561–566, 1998

A method for analysing and comparing treatment planning system (TPS) data and ferrous dosimeter gel measurements evaluated with MRI (FeMRI) was developed, including image processing to final absorbed dose images. Measurements were analysed according to this method and FeMRI data were thereby compared with the TPS-calculated dose distribution. For photons, differences between FeMRI- and TPS dose data were mainly within ±2%. Minor shortcomings found in both the FeMRI system and the TPS are explained and discussed. For electron beams, there was an overall good agreement. It was found that the TPS underestimates the lateral scattering dose outside the primary beam, but the reported dose difference corresponds to a small spatial deviation (less than 2 mm). It is important to consider this single beam data comparison when the method is extended to more complicated situations, for example when using several beams.

Received 22 December 1997
Accepted 22 May 1998

It is important to verify dose calculations in order to carry out an optimal radiotherapy. Treatment planning systems (TPS) are under continuous development with the implementation of improved dose calculation models, which may require new verifications (1). Most dosimetry techniques are incapable of 3D measurements. Ionization chambers and semiconductor detectors are often limited to be used in water tanks. Other methods (for example film or thermoluminescent dosimeters, TLD) can be used with anthropomorphic phantoms, but these methods are time-consuming, and can present fundamental dosimetric problems such as energy dependence. A soft tissue equivalent 3D dosimetry system would be of great value in the validation of treatment plans. The complete dose distribution in various treatments can be measured with a single fraction.

The agarose gel system used, based on ferrous sulphate and evaluated with MRI (FeMRI) has proved to be a detector with a total uncertainty in the same order of magnitude as other commonly used detectors (2).

Although ferrous sulphate dosimeter gel (FeMRI) has been used for TPS verification in some clinical cases (3–5), single beam verification data are rare. Deviations in basic dose data measured by FeMRI and compared with TPS data could be propagated and very difficult to identify and separate when several beams and/or beams of different radiation quality are used.

The purpose of this study was to develop a method for comparison of two-dimensional (dose matrix) TPS-calculated data with the corresponding FeMRI-measured data. To evaluate the possible limitations of FeMRI in verification of a TPS, we used only basic irradiation geometries (single beam). The whole clinical chain, including CT scanning, dose planning and irradiation set-up, was included in the dose verification using FeMRI. The discrepancies between FeMRI and TPS data and possible consequences when the method is extended to more complicated treatment regimes are discussed.

An alternative to a ferrous-based dosimeter gel is to use a monomer solution with a high concentration of a cross-linker together with and a gelling agent. The radiation-induced polymerization can also be evaluated using MRI (PoMRI) (6, 7). Unlike the FeMRI systems, the PoMRI method is not affected by diffusion of the radiation-

 ISSN 0284-186X

induced products. However, utilising the beams and the MRI acquisition protocol proposed in this study, the FeMRI system can be used without significant blurring of the dose distribution that is caused by diffusion (8).

MATERIAL AND METHOD

Gel preparation, phantom and MRI-evaluation

The preparation of the ferrous sulphate dosimeter gel was based on a previously described method (9). The gel was poured into a cylindrical perspex phantom, 15 cm in diameter and 13 cm in height. The cylindrical side walls were 5 mm thick, and the circular bottom of the phantom was 2 mm thick (i.e. the beam entrance window). The MRI acquisition of each phantom was performed twice (i.e. one evaluation before and one after irradiation) to enable background subtraction (Fig. 1). This was done in order to decrease the effects resulting from non-uniformity of the MRI image plane. The MRI-scanner used throughout this work was a Philips ACS II 1.5 T, and all the scans were carried out using the head coil. An MRI-acquisition protocol consisting of a spin-echo sequence using two different repetition times (TR = 200 ms and TR = 1700 ms) was used in order to give an accurate calculation of T1, pixel by pixel (Table 1). The acquisition protocol is the result of optimization studies in stochastic noise level in the calculated T1-image (10, 11).

Irradiation and treatment planning

The dosimeter gel-filled phantom was irradiated using a Philips Linac SL75/20 linear accelerator. Two irradiation examples were studied—a single 10 MeV electron beam and a single 5 MV photon beam. The 10 MeV electron beam irradiation was performed using a field size of 7×7 cm^2 and a source to surface distance (SSD) of 95 cm. The 5 MV photon beam irradiation was carried out using the field size 8×8 cm^2 and SSD = 100 cm. The absorbed dose distributions for these irradiations were calculated using a TPS, capable of performing 3D dose distribution calculations (TMS™-Radix 2.9C, Helax®, Uppsala, Sweden). Before planning, the gel-filled phantom was CT-scanned and the image data transferred to the TPS for calculation of the electron density matrix. In order to make the calculated two-dimensional dose information available for digital comparison, the complete absorbed dose matrix had to be exported from the TPS using the hard-copy file export routine of TMS™-Radix. The distance between the calculation points was 2.3 mm in our geometry, and the matrix size 63×50 pixels, the field of view thereby covering the main part of the phantom.

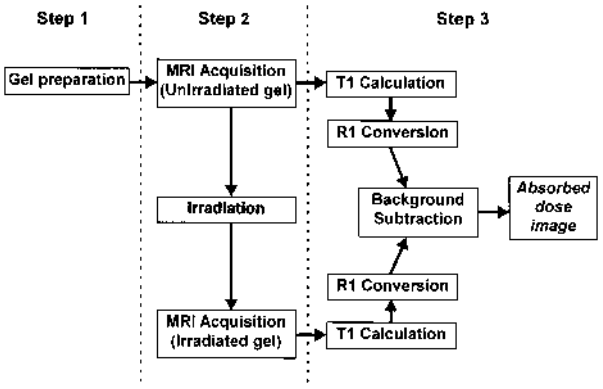

Fig. 1. The evaluation procedure of the FeMRI dosimeter gel system.

Table 1

Parameters of the MRI-acquisition protocol including two spin-echo sequence scans with different repetition times

Scan Number	1	2
Echo time (TE) (ms)	12	12
Repetition time (TR) (ms)	200	1700
Number of excitations	8	2
Field of view (FOV) (mm^2)	300×300	300×300
Matrix size (pixels)	256×256	256×256
Slice width (mm)	15	15

Agreement between the calculated absorbed dose matrix and one-dimensional data was confirmed by generating a separate horizontal line dose profile with a spatial resolution of 1 mm for the 10 MeV electron beam using the line dose routine of TMS™-Radix (12).

Image processing

The MR images from the MRI scanner were first transferred to a PC computer where the image header and T1 calculation were removed with a specially designed Microsoft® Windows 95™ program (13). The resulting T1 images were then transferred to an Image Processing System (IPS) (hardware: Digital DEC station 5000/240 and software: Analyze™, Mayo Clinic, Rochester, USA) where all the subsequent image processing of the T1 images was performed. The absorbed dose matrix images exported from the TPS were transferred directly to the IPS.

Dosimeter gel images. Using the IPS, all the T1 images were converted to R1 images (R1 = 1/T1). This conversion includes addition of the integer 1 to the image pixel values to avoid division by zero, and a division where the integer 10^6 is divided by the image pixel values. The integer 10^6 was selected to ensure an adequate R1 range (the T1 range is approximately 100–1000 ms). The background R1 images were then subtracted from the irradiated R1 images (Fig. 1). All background subtracted R1 images were rotated by an angle of 0.75°, because of the phantom not being aligned with the main axes in the MR images. This rotation procedure included pixel position interpolation. The rotated image was then normalized to a relative dose

distribution image. For the 10 MeV electron beam the normalization point was at dose maximum (22 mm depth), and for the 5 MV photon beam at 50 mm depth. The lateral position of the normalization point was at the centre of the radiation beam for both radiation qualities. The R1 value in the normalization point was measured using a small 3×3 pixel ROI. The normalization included a multiplication of the integer 10^3 with the pixel values of the background subtracted image and a division by the R1 value measured at the normalization point. The pixels outside the inner surface of the phantom are of no interest. The 256×256 pixel image was therefore truncated to a new 122×97 pixels image which only contains pixels inside the phantom, i.e. pixels with absorbed dose information. The pixel size was 1.15×1.15 mm^2.

TPS images. Using the IPS, the 63×50 pixel absorbed dose matrix from the TPS was expanded to a 122×97 pixel image. The image was then normalized in the same manner as the corresponding dosimeter gel image, using the corresponding normalization points.

Matching the TPS image to dosimeter gel image. To compare the dose image from the TPS with the corresponding dosimeter gel dose image, the two images were spatially matched in the lateral direction. Matching in the depth dose direction was unnecessary because all the distances being well defined in this direction. Therefore, the errors in irradiation set-up in this direction are negligible. The landmark in the two dose images coinciding after the matching procedure was the point along the 50% dose level on the right-hand side of the dose distributions, positioned at the same depth as the normalization point. The matching procedure was restricted to one side only in order to exclude errors attributable to the irradiation field size set-up, and consisted of a lateral translation of the TPS distribution 3 pixels for the 10 MeV electron beam and 1 pixel for the 5 MV photon beam. The uncertainty of the matching procedure is difficult to predict.

In our case the main limitation is probably determined by the pixel size.

After the matching procedure, one depth dose curve and one horizontal line profile were obtained from both the TPS dose images and the dosimeter gel dose images, positioned to intersect with the normalization points. The penumbra widths of the calculated and the measured dose distribution were determined using the horizontal line profiles.

Isodose curves were also obtained from the TPS dose images and dosimeter gel dose images using the pixel value threshold function of the IPS.

RESULTS

The central depth dose curves, the horizontal dose profile curves and the isodoses originating from the TPS-calculated and the FeMRI-measured dose matrix were compared for the 10 MeV electron (Figs. 2 and 4a) and the 5 MV photon (Figs. 3 and 4b) beams.

The horizontal dose profile produced using the line dose data export from the TPS was, as expected, found to agree with the TPS calculated dose matrix data (Fig. 2b).

For the electron beam, the FeMRI- and the TPS data were in very good agreement in the central region of the beam (Figs. 2 and 4a). At shallow depths, differences of up to 3% were found (Fig. 2a). The TPS input data are measured using a semiconductor detector and differences of the same order were found when comparing FeMRI with a semiconductor detector system (2). This indicates underestimation of the contribution of scattered electrons close to the surface using both a semiconductor detector and the TPS. In the penumbra regions (Fig. 2b), differences of up to 5% were found, and the corresponding penumbra widths also differed significantly, 3.7 mm (Table 2). Similar deviations have also been reported elsewhere (14) and can be explained by the way the TPS handles the lateral scatter of the electrons outside the primary beam. However, these discrepancies (best seen in Fig. 4a) were found in a region exhibiting a very steep dose gradient and therefore correspond to a small geometric displacement of the absorbed doses, less than 2 mm.

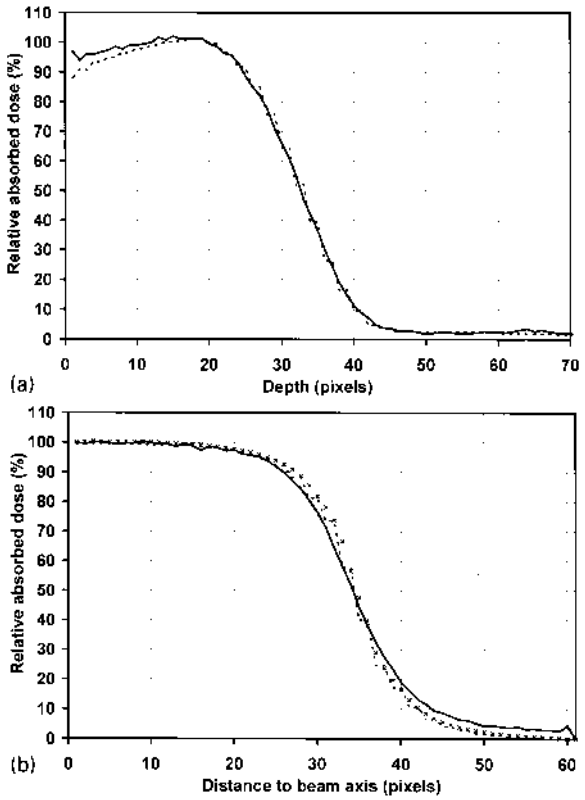

Fig. 2. Depth doses (a) and horizontal line profiles (b) for the 10 MeV electron beam obtained from the dosimeter gel dose image (–), from the TPS dose image (– –) and from the TPS line dose routine (×).

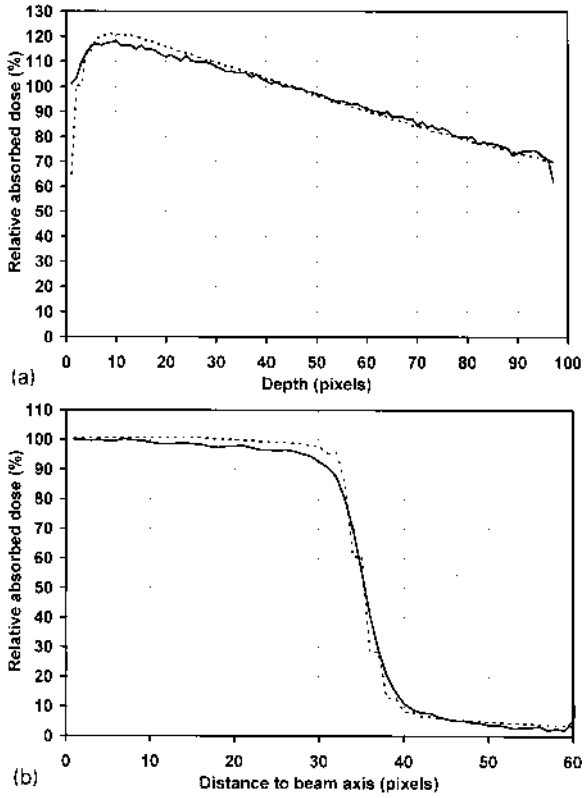

Fig. 3. Depth doses (a) and horizontal line profiles (b) for the 5 MV photon beam obtained from the dosimeter gel dose image (–) and from the TPS dose image (– –).

Thus, the FeMRI system has good overall capability in TPS electron dose distribution verification.

For photons, the TPS system is known to be very accurate (15), but there are some shortcomings in the build-up region and at greater depths (16). The differences between FeMRI- and TPS data (Fig. 3a and Fig. 4b) near the surface ($< 4\%$) cannot be fully explained by the shortcomings of the TPS system. FeMRI seems to measure a lower dose than predicted by other detector systems (2).

Differences at greater depths, indicating that the TPS system underestimates ($< 2\%$) the absorbed dose, are in accordance with the results found by Knöös et al. (16). No significant deviations (< 1.5 mm) were found when comparing the widths of the penumbra region (Table 2).

Thus, FeMRI has good overall capability in TPS photon dose distribution verification, although at shallow depths some limitations in the FeMRI system have been found.

DISCUSSION

A dosimeter gel system can be used to measure complicated treatments, including several beams of various qualities in a single fraction. The optional phantom shape and the tissue equivalence of the gel are other properties that make FeMRI an interesting verification tool. A deviation matrix resulting from subtracting the calculated dose matrix from the FeMRI measured dose matrix could also be used to evaluate the application. For visualization purposes, the deviation matrix could be coded using a colour scale (5).

The differences between the TPS- and FeMRI data found in this study could be of importance when utilizing

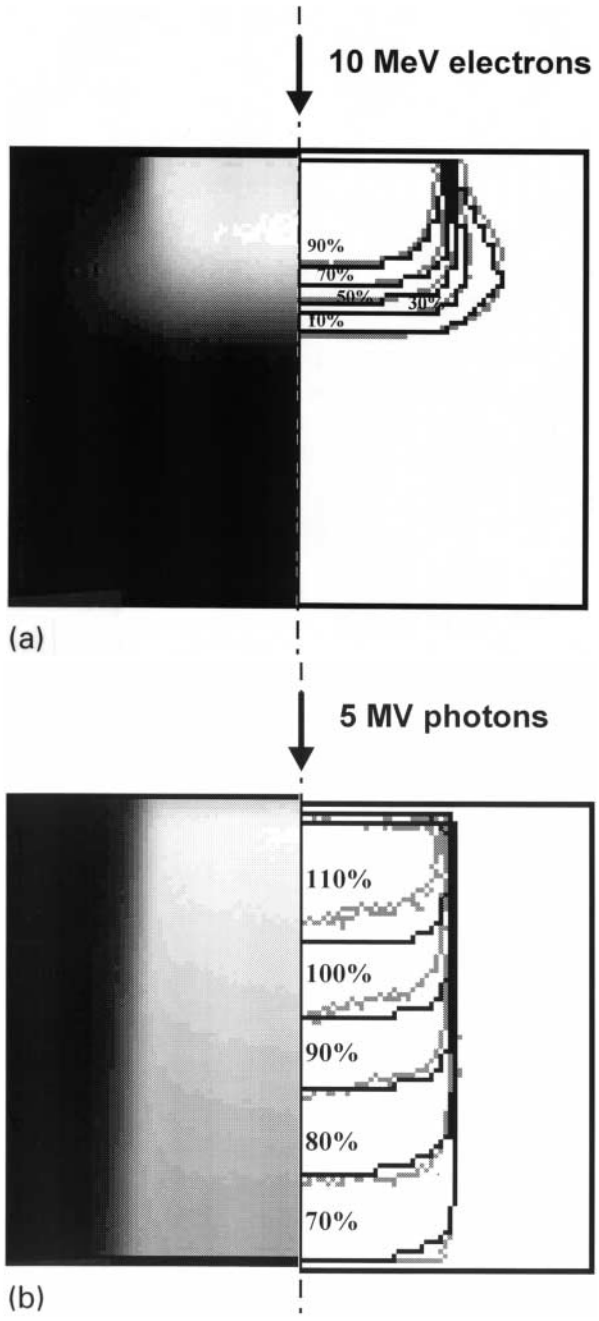

Fig. 4. Isodose curves (right side) for the 10 MeV electron beam (a) and the 5 MV photon beam (b) obtained from the dosimeter gel dose images (grey lines) and from the TPS dose images (black lines). The dosimeter gel dose image from which the dosimeter gel isodoses are obtained is also presented (left side).

Table 2

Estimated penumbra widths (90%–10%, dose maximum) in mm for 5 MV photons (8×8 cm^2) and 10 Mev electrons (7×7 cm^2)

Tool	Detector size (mm)	5 MV	10 MeV
Dosimeter gel	The pixel size is 1.15×1.15 mm^2	8.5	18.4
TPS calculated	–	7.0	14.7

a verification with several beams of different radiation quality. To interpret such a verification, the deviations between the TPS and FeMRI of the individual beams are of great value. The deviations could have different origins, as shortcomings of both detector and TPS system. Deviations can be enhanced or cancelled, particularly if several treatment beams are superimposed (5). Hence, before setting up complex treatment techniques using FeMRI, it is very important to investigate the dosimetry system in simple and well-defined radiation beams. In addition, uncertainties are always introduced when comparing different absorbed dose determination methods as a TPS and a verification system. Questions arise about what criteria should be used when evaluating deviations over a volume and about difficulties in displaying the deviation in a relevant way (14). The use of a dose volume histogram (DVH) has been proposed (5). The unique possibilities of 3D gel detectors and MRI are obvious here; no other detector system can produce such a 3D representation of a potentially complex measured dose distribution, but the whole volume of interest has to be MR evaluated to reach a true DVH comparison. Other comparison methods proposed are dose difference plotted against the complete evaluated volume (17) or evaluation of different regions in relation to the beam edges (18). FeMRI can be used to evaluate deviations in optional volumes just by changing the size of the ROI in the deviation images and can be generalized to several slices and larger volumes (as well as the 3D TPS calculations). The dose matrix-based data (TPS and FeMRI) facilitate pixel by pixel verification.

Even though the FeMRI system itself today has a total uncertainty better than 3% (2), one must bear in mind the spatial uncertainty of about ± 1 mm when comparing specific pixels obtained by the TPS and FeMRI methods. In addition, one should be aware of the inherent geometrical limitations of using both CT (the TPS calculations are based on CT information) and MR scanners. It is essential to have high quality equipment and, in particular, there are certainly specific requirements for MR scanners used in MRI dosimetry. This will be reported in a separate study. However, in order to be a useful tool in quality assurance, the detector must be able to detect differences of 2% or 2 mm positional error (1, 19). The present FeMRI system has the potential to fulfil these requirements (2).

Sophisticated matching procedures, often used in, for example, stereotactic treatment (fusing MRI, CT and PET images), could be implemented to improve the accuracy in a true 3D verification. External references have to be present in the images in order to reach an optimum matching. Further studies will improve this feature, which is important when using FeMRI in stereotactic treatment. In this study, using the complete absorbed dose distribution, no landmarks other than the edges of the phantom and the outer definitions of the beams were used to correlate the matrices (as described in Section 2.3).

CONCLUSION

A method for analysing and comparing TPS- and FeMRI dose images was developed, including image processing to the final absorbed dose images. The method can readily be generalized into a 3D comparison. FeMRI for TPS dose verification in basic irradiation geometries has proved to be a useful dosimetric tool. Minor shortcomings in both the FeMRI system and the TPS were found. Nevertheless, the TPS system investigated in this study was found to be accurate and well within the limits stated by the ICRU 42.

In order to extend the method to investigate complex multi-beam treatments and full 3D calculations, this study and other single beam data comparisons are of great value in accomplishing a more complete interpretation of the results.

ACKNOWLEDGEMENTS

This work was supported by the Swedish Cancer Foundation project number 2349-B96-08XAA, the Cancer Foundation of Malmö University Hospital and FMC Bioproducts Europe, Denmark. The authors express their thanks to Christina Vallhagen Dahlgren, University Hospital, Uppsala, for assistance with treatment planning.

REFERENCES

1. Van Dyk J, Barnett RB, Cygler JE, Shragge PC. Commissioning and quality assurance of treatment planning computers. Int J Radiat Oncol Biol Phys 1993; 26: 261–73.
2. Johansson Bäck SÅ, Magnusson P, Fransson A, et al. Improvements in absorbed dose measurements for external radiation therapy using dosimeter gel and MR imaging (FeMRI). Phys Med Biol 1998; 43: 261–76.
3. Olsen DR, Hellesnes J. Absorbed dose distribution measurements in brachytherapy using ferrous sulphate gel and magnetic resonance imaging. Br J Radiol 1994; 67: 1121–6.
4. Chan MF, Ayyangar KM. Confirmation of target localization and dosimetry for 3D conformal radiotherapy treatment planning by MR imaging of a ferrous sulfate gel head phantom. Med Phys 1995; 22: 1171–5.
5. Johansson SÅ, Magnusson P, Fransson A, et al. Dosimeter gel and MR imaging for verification of calculated dose distributions in clinical radiation therapy. Acta Oncol 1997; 36: 283–90.
6. Maryanski MJ, Gore JC, Kennan RP, Schulz RJ. NMR relaxation enhancement in gels polymerized and cross-linked by ionizing radiation: a new approach to 3D dosimetry by MRI. Magn Reson Imaging 1993; 11: 253–8.

7. Maryanski MJ, Ibbott GS, Eastman P, Schulz RJ, Gore JC. Radiation therapy dosimetry using magnetic resonance imaging of polymer gels. Med Phys 1996; 23: 699–705.
8. Olsson LE, Arndt J, Fransson A, Nordell B. Three-dimensional dose mapping from gamma knife treatment using a dosimeter gel and MR-imaging. Radiother Oncol 1992; 24: 82–6.
9. Olsson LE, Appleby A, Sommer J. A new dosimeter based on ferrous sulphate solution and agarose gel. Appl Radiat Isot 1991; 42: 1081–6.
10. Prato FS, Drost DJ, Keys T, Laxon P, Comissiong B, Sestini E. Optimization of signal-to-noise ratio in calculated T1 images derived from two spin-echo images. Magn Reson Med 1986; 3: 63–75.
11. Helmius E. A study of the combinations of repetition times in a spin echo measurement for the estimation of the longitudinal relaxation time least sensitive to noise. MSc Thesis. Stockholm: Department of Radiation Physics, Stockholm University, 1993.
12. Montelius A, Jung B, Rikner G, Murman A, Russel K. Quality Assurance Tests of the TMS–Radix Treatment Planning System. Advanced Radiation Therapy Tumor Response Monitoring and Treatment Planning 1992; 523–7.
13. Magnusson P, Johansson SÅ, Olsson LE. PMRelax for Windows: A general program for calculations of relaxation times in MR imaging. Report MA RADFYS 95:05. Malmö: Department of Radiation Physics, Lund University, 1995.
14. Blomquist M, Karlsson M, Karlsson M. Test procedures for verification of an electron pencil beam algorithm implemented for treatment planning. Radiother Oncol 1996; 39: 271–86.
15. Ahnesjö A, Saxner M, Trepp A. A pencil beam model for photon dose calculation. Med Phys 1992; 19: 263–73.
16. Knöös T, Ceberg C, Weber L, Nilsson P. The dosimetric verification of a pencil beam based treatment planning system. Phys Med Biol 1994; 39: 1609–28.
17. Fraass BA, Martel MK, McShan DL. Tools for dose calculation verification and QA for conformal therapy treatment techniques. In: Hounsell AR, Wilkinsson JM, Williams PC, eds. Proceedings of the XIth international conference on the use of computers in radiation therapy. Manchester, 1994: 256–7.
18. Stern RL, Fraass BA, Gerhardsson A, McShan DL, Lam KL. Generation and use of measurement-based 3-D dose distributions for 3-D dose calculation verification. Med Phys 1992; 19: 165–73.
19. ICRU. Use of computers in external beam radiotherapy procedures with high-energy photons and electrons. ICRU Report 42. Bethesda (MD): ICRU, 1987.